On the possible generalizations of the Kitagawa–Takahashi diagram and of the El Haddad equation to finite life

M. Ciavarella *, F. Monno

CEMeC – Centre of Excellence in Computational Mechanics, Policlinico di Bari, Viale Japigia, 182, Politecnico di Bari, 70125 Bari, Italy

Abstract

The celebrated Kitagawa–Takahashi (KT) diagram, and the El Haddad (EH) equation, have received great attention since they define quite successfully the region of non-propagation (or the condition of self-arrest) for short to long cracks. The EH equation can be also seen as an "asymptotic matching" between the fatigue limit and the threshold of crack propagation. Above this curve, finite life is expected, since cracks propagate and eventually lead to final failure. In this paper, possible extensions of the EH equation to give the life of a specimen with a given initial crack as a function of the applied stress range, using only "asymptotic matching" equation between known regimes, namely the Wöhler SN curve (or some simplified form, like Basquin law), and the crack propagation rate curve (or just the Paris' law). This permits an extension of the so-called "intrinsic crack" size concept in the EH equation for infinite life. The generalized El Haddad equation permits to take into account approximately of some of the known deviations from the Paris regimes, for short cracks, near the fatigue threshold or fatigue limit, or to the static failure envelope. The new equations are also plotted as SN curves, showing that power-law regimes seem very limited with many possible deviations and truncations, even when the crack propagation law has a significant power-law regime. The diagram remains partly qualitative (for example, we neglect geometric factors), and can be considered a first attempt towards more realistic maps. Particularly interesting are the cases with the Paris exponent $m < 2$, in which propagation tends to be very slow until very close to the toughness failure, making the maps qualitatively different.
© 2006 Elsevier Ltd. All rights reserved.

Keywords: Fatigue; Notches; Cracks; Initiation; Fatigue life

1. Introduction

The Kitagawa–Takahashi (KT) diagram [1] (see Fig. 1) is today one of the most used simple criteria and graphical aid to either qualitatively understand the behavior of short-cracks or design for infinite life taking into account of the presence of (at least) two thresholds of fatigue, that given by the classical stress-based fatigue limit, $\Delta\sigma_0$, and that given by the more recently introduced threshold stress intensity range ΔK_{th} of Paris' crack propagation law [2,3], relating the crack growth rate, da/dN, to the amplitude of the applied stress intensity factor, ΔK. Clearly, the KT diagram simply visualizes the condition from non-propagation, or the condition for self-arrest of cracks – the two possible interpretations depend also on how the threshold is defined and measured, since the crack tip plasticity depends on the loading history. The fatigue threshold in fatigue ΔK_{th} differs from the more classical corresponding material property (fatigue limit $\Delta\sigma_0$) by a square root of a length scale, and the transition size is immediately defined from dimensional analysis as the constant a_0:

$$a_0 = \frac{1}{\pi}\left(\frac{\Delta K_{th}}{\Delta\sigma_0}\right)^2, \tag{1}$$

which of course is the "El Haddad" length scale [4]. Some empirical equations are for example discussed in the recent paper by Atzori et al. [5]. In the present paper, we shall consider, as example, a few steels whose properties are described in Table 1. SAE1045 is a medium carbon steel used

Nomenclature

a_f	final size of the crack
$a_{f,t}$	final size of the crack in the transition from Basquin to Paris dominated regime
a_i	initial size of the crack
a_t	transition size of the crack from Basquin to Paris (or Donahue) dominated regime
a_0	transition crack size for infinite life in El Haddad equation (or "intrinsic crack")
a_0^S	transition crack size in the "El Haddad" equation equivalent for static failure
b	fatigue strength exponent in Basquin's law
C	constant in Paris's law
$\overline{C}$	constant in Basquin's law
da/dN	crack growth rate or advancement per cycle
k	exponent in Basquin's law
m	exponent in Paris's law
N	number of cycles to failure
N_0	number of cycles of transition from static behaviour to SN curve (in the schematic Basquin law)
N_∞	infinite life (10^7 in the following)
N_t^i	transition from Paris to Basquin dominated regime for $a_i/a_0 = i$
$N_{t,\infty}^i$	transition from Paris to El Haddad dominated regime for $a_i/a_0 = i$
R	stress ratio, ratio between minimum and maximum stress

v_a	advancement per unit cycle in Paris' power law ($v_a = da/dN$)
v_a^c	advancement per unit cycle in Paris' power law when $\Delta K = K_{Ic}(1 - R)$
v_a^{th}	advancement per unit cycle in Paris' power law when $\Delta K = \Delta K_{th}$
ΔK	stress intensity factor range
ΔK_{th}	threshold stress intensity range
$\Delta K_{th,sc}$	threshold stress intensity range corrected for short cracks
$\Delta\sigma_{EH}$	El Haddad threshold of stress range
$\Delta\sigma_{EHS}$	equivalent El Haddad threshold of stress range for static life
$\Delta\sigma_{EHG}$	generalized El Haddad threshold stress range for finite life
$\Delta\sigma_{lim,th}$	fatigue limit stress range derived from the threshold stress intensity range
$\Delta\sigma_{KT}$	Kitagawa–Takahashi threshold of stress range
$\Delta\sigma_{KTG}$	generalized Kitagawa–Takahashi threshold of stress range for finite life
$\Delta\sigma_R$	stress range at static failure
$\Delta\sigma_t$	transition stress range from Basquin to Paris dominated regime
$\Delta\sigma_0$	stress range at fatigue limit
K_{Ic}	fracture toughness
σ_f'	fatigue strength coefficient

in gears, shafts, axles, bolts, studs, and various machine parts.

Many examples of applications of the KT diagram exist, Refs. [6–8] discuss weld metals, foreign-object damage and fretting fatigue, respectively. Also, based on the KT-diagram, various generalized diagrams have emerged for

Fig. 1. The KT diagram and the El Haddad equation for example steel 1045 material (see Table 1) $R = -1$.

design [9–11]. A particularly interesting "fatigue damage map" of applied stress range vs. crack length is defined in [11], including 5 areas: (i) crack arrest, (ii) stage I (or short crack) growth, (iii) stage II or long crack growth, (iv) stage III and (v) toughness failure. The crack arrest zone is defined not with the El Haddad equation (although the latter is eventually found to better correlate with experiments), but with a combination of models of dislocations at crack tip competing with micro structural barriers (requiring information on grain size, crack closure stress and grain orientation factors), with empirical equations for R-ratio dependence of ΔK_{th}. The stage I (short crack) propagation is then described with crack tip plasticity models, whereas the transition stage I–stage II (where Paris law can be reasonably be used) is supposed to occur when crack is long enough that plasticity is accommodated on two grains without further growth of the crack. Finally, equations and models for stage III propagation and final toughness failure (or general yielding) are given. It is clear, however, that this approach requires many material constants that are not available in general, and, anyway, we are rather interested in a more "design-oriented" map, giving information of the life (actual number of cycles) of a specimen for a given stress range and initial size of the crack. This is perhaps close to the ideas towards the end
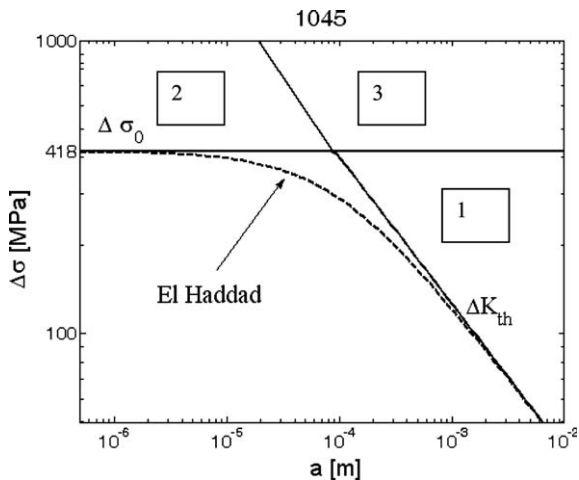
Table 1
Mechanical properties of some steels[a]

Material	Stress units	UTS	Yield strength	Fatigue strength coeff	Fatigue strength exponent	Crack growth coeff (CGC)	CGC units/cycle	Crack growth exponent	Thresh SIF $R = 0$	Fracture toughness
1045	MPa	621	382	948	−0.09	8.20E − 13	m	3.5	7.1	80
A588	MPa	480	355	1036	−0.123	4.02E − 12	m	3.6	5.2	73
RQT501	MPa	590	472	892	−0.089	1.00E − 10	m	1.72	5.35	80
RQT701	MPa	825	735	955	−0.063	1.00E − 10	m	1.72	5.35	113

[a] From Multiaxial Fatigue, Analysis and Experiments, Eds. G.E. Leese, D. Socie, SAE Pub. AE-14, 1989. Also, in Fatigue Calculator in the site http://www.fatiguecalculator.com/ and ref. therein.

of the overview paper on fatigue by Fleck et al. [12], where a map is given of the allowable stress range for a given life and initial crack size, for various materials, as obtained by the simple integration of Paris' law.

The present paper shall try to pursue a simple strategy, and in particular define a hybrid "damage tolerant/safe-life" design procedure without detailed information or advanced models on the short crack behavior. We shall start by investigating on the integrated form of Paris law as it looks in the Kitagawa–Takahashi diagram. Subsequently, in order to obtain a life prediction consistent with other information on the SN data, a "matching asymptotic" interpolation procedure is suggested. The idea comes from the example of the infinite life case, for which the El Haddad empirical equation [4], is a simple immediate solution based on "matching" the asymptotic behavior of the fatigue limit regime (for absence of the crack) to the threshold regimes governed by the a_0 constant (for long cracks), interpolating as (see also Fig. 1)

$$\Delta\sigma_{EH} = \Delta K_{th} / \sqrt{\pi(a + a_0)}, \qquad (2)$$

which suggests the perhaps misleading definition of a_0 as the "intrinsic crack". Notice that geometrical factors are not included in this equation, which implies that we suppose the same definition of a_0 intrinsically considered in (1) holds. The El Haddad equation (2) defines a simple threshold for crack propagation (or self-arrest), and hence divides the map into a lower "safe-life" no-damage area, and an upper crack propagation area of finite life, on which we shall now concentrate our interest. We expect finite life either because the LEFM threshold condition is over passed for a large initial crack (Fig. 1, area indicated as "1") giving directly a true stage II propagation, or because the stress level is high enough for the initiation (i.e. short crack or stage I propagation), and later propagation of cracks (area indicated as "2" in the figure). A more complex region is "3", where both the fatigue limit and the fatigue thresholds are over passed.

The first area ("1") is likely to be correctly and relatively easily modeled with Paris' law (at most, with possible deviations near the fatigue threshold, as we shall see below), whereas the second ("2") is not, since there is a delicate interplay of initiation and propagation of short cracks: propagation occurs also *below* the (long crack) threshold (see Suresh [13]). Also, the propagation rate of short crack

is driven by a much higher power law of the stress range than in the Paris law (Polák [14], Murakami et al. [15,16], Nisitani et al. [17,18]). The dependence on the crack size is not the power law of exponent $m/2$ as in Paris but a linear law, suggesting the resulting SN curve has generally a milder dependence on initial crack size. However, this linear dependence, may be perhaps still an intermediate behaviour and for very small cracks, it could further reduce to no dependence at all, as would be expected from a Basquin–Wöhler-like SN law. Here, we shall assume that region "2" for very small cracks is indeed appropriately modelled with a Basquin–Wöhler-like SN law, as in the traditional approach to fatigue. Finally, region "3" is where more elaborated effort is needed, and where the originality of the present paper is concentrated. The idea is to generalize the concepts behind the El Haddad equation, i.e. the use of "asymptotic matching" between two known regimes.

Notice that an immediate extension of the definition of the infinite life "intrinsic crack" size a_0, is the corresponding static equivalent a_0^S, defined as a function of K_{Ic}, the toughness of the material, and σ_R its tensile strength as:

$$a_0^S = \frac{1}{\pi}\left(\frac{K_{Ic}}{\sigma_R}\right)^2, \qquad (3)$$

which incidentally can be used to define the "equivalent" of the El Haddad equation for static life

$$\Delta\sigma_{EHS} = \Delta K_{Ic} / \sqrt{\pi(a + a_0^S)}. \qquad (4)$$

Hence, if the size a_0 is the order of magnitude of the crack in the material which does not alter the fatigue properties of it, and the corresponding static equivalent a_0^S, is the size of crack which does not alter significantly the static properties of the material, then an intermediate size a_t, could be the size of the crack which doesn't alter the strength of the material to a certain, finite life N. An implication is that the definition of "short crack" should be generalized accordingly. In particular, "short" is nearly always related to the fatigue limit and fatigue threshold (i.e. from the El Haddad intrinsic crack a_0), whereas the definition of "short" is more correctly done with respect to the size of the process zone, and hence should also depend on the load level — in the limit of static failure, the size a_0^S, often orders of magnitude larger than the El Haddad size, is the correct

definition of "short". Hence, what is short for static failure is mostly likely "long" around the fatigue limit region. This reflects the interplay of various mechanisms: certainly, the interaction occurring between fatigue threshold limit and fatigue limit (for example, crack self-arrest at grain boundaries), is not the same as that between yield static failure and toughness failure at static life.

2. Classical equations for initiation and propagation in fatigue

2.1. SN curve equations

The Wöhler SN curve gives us at low load levels, High Cycle Fatigue (HCF), and at higher load levels, Low Number of Cycles (LCF), with the cyclic plastic deformation certainly assuming a more relevant role at higher and higher stress levels.[1] This empirical Wöhler curve will be assumed to be of the power law "Basquin" type, of the form:

$$N_0 \Delta \sigma_R^k = N_\infty \Delta \sigma_0^k = N \Delta \sigma^k = \overline{C} \quad N_0 < N < N_\infty, \tag{5}$$

where $\Delta \sigma_R = \sigma_R (1 - R)$ is the range of stress at static failure, $\Delta \sigma_0$ the fatigue limit and $\Delta \sigma$ is the stress range for having a life N; also, N_0, and N_∞ are the number of cycles as defined in Fig. 2 (notice that, for simplicity, we consider the single case of $R = -1$ ratio here, with different ratios requiring accordingly modifications in the constants). Basquin law can also be written in the notation of the Coffin–Manson equation, of which it is the elastic part only, as

$$\Delta \sigma / 2 = \sigma_f' (2N)^b, \tag{6}$$

where σ_f' is called fatigue strength coefficient, b is fatigue strength exponent, and $2N$ the number of reversals.[2] Notice that, in Eqs. (5) and (6), we intend for N (or $2N$) the number of cycles (or reversals) to failure.

Moving to the region where *both* fatigue limit and fatigue threshold are over passed (i.e. in the range "3" in the diagram of Fig. 1), we start already from a condition *above* the threshold in the Paris diagram, but for the same applied stress range we expect a faster propagation than the equivalent condition of stress intensity factor range of region "1", deviating from the original Paris' law prediction.

2.2. Crack propagation equations

Turning to the crack propagation issue, the celebrated Paris's power law [2,3] gives the advancement da of fatigue crack per unit cycle dN, v_a, as a function of the amplitude of stress intensity factor ΔK (see Fig. 3) as:
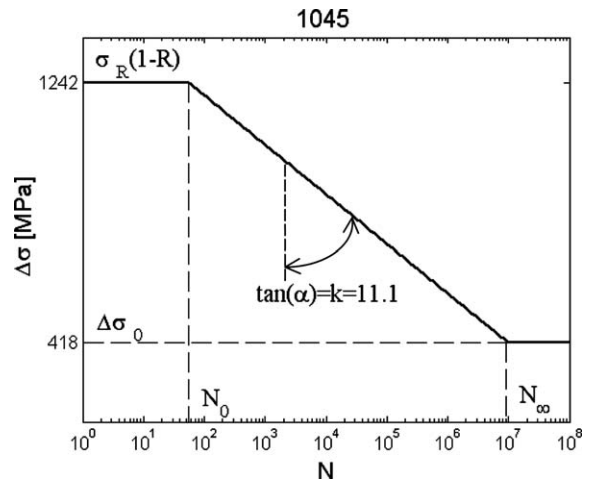

Fig. 2. The schematic Basquin–Wöhler law (5) for example steel material (see Table 1).

$$v_a = \frac{da}{dN} = C \Delta K^m, \quad \Delta K_{th} < \Delta K < K_{Ic}, \tag{7}$$

where ΔK_{th} is the "fatigue threshold", and K_{Ic} the "fracture toughness" of the material; C and m are the so-called Paris' constants. There is therefore dependence on dimension of the crack and on stress range level only via the stress intensity factor range $\Delta K = Y \Delta \sqrt{\pi a}$, where Y is a geometrical factor. The law is mostly valid in the range 10^{-8} to 10^{-6} m/cycle, intersecting ΔK_{th} at about $v_a^{th} = 10^{-9}$ m/cycle.

To compute the life of a distinctly cracked specimen having an initial crack size a_i, then, in the simplest case of constant remote stress and removing possible variations of geometrical factor (and even further simplifying, assuming $Y = 1$), for $m \neq 2$ we integrate (7) to get:

$$a_i^{2-m/2} - a_f^{2-m/2} = \left(\frac{m-2}{2} \right) C \pi^{m/2} \Delta \sigma^m N, \tag{8}$$

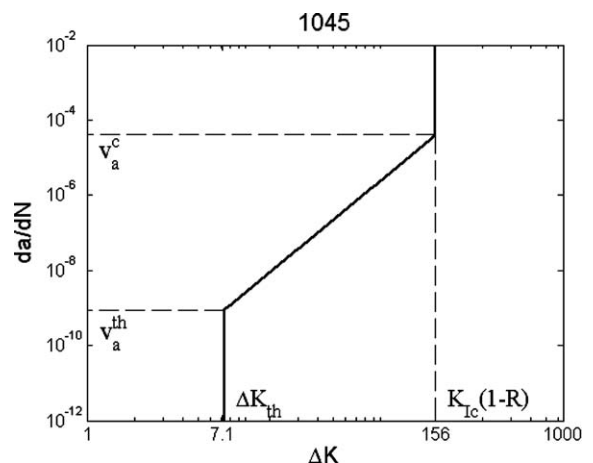where integration is done up to the final size of the crack, which by definition is obtained for toughness failure

Fig. 3. Paris law: schematic form (7) for example steel material (see Table 1) SAE1045. We assumed here $R = -1$.

---

[1] For strain controlled experiments, it is possible to use the total strain approach, where the sum of Coffin–Manson law for the plastic strains, and of the Baquin law for the elastic strains. is used to predict fatigue life.

[2] To convert Eq. (6) into the notation of Eq. (5), just notice that $b = -1/k$ and hence $\overline{C} = (2\sigma_f')^k / 2$.

$$a_\mathrm{f} = \frac{1}{\pi}\left(\frac{K_\mathrm{Ic}(1-R)}{\Delta\sigma}\right)^2. \tag{9}$$

Often, the dependence on the final size of the crack a_f (9) is removed on the grounds that $a_\mathrm{f} \gg a_i$ (for $m > 2$) and hence it is relatively not influent away from the toughness failure region. In this case

$$a_i^{2-m/2} = \left(\frac{m-2}{2}\right)C\pi^{m/2}\Delta\sigma^m N. \tag{10}$$

It is interesting, however, to remark that this is an "equivalent" SN fatigue curve which depends on the initial crack size, a_i. Notice also that the threshold condition for infinite life (which we could define, conventionally, at $10^{\wedge}7$ cycles) obtained from Eq. (10) would tend not to coincide with that directly obtained from the threshold value which also depends on a_i but with a different power:

$$\Delta\sigma_\mathrm{lim,th} = \frac{\Delta K_\mathrm{th}}{\sqrt{\pi a_i}}. \tag{11}$$

In practise, when we use the integrated form of Paris law ((8) and (10)), we shall truncate the equation to the fatigue "limit" defined by Eq. (2), and this truncation will not occur at $10^{\wedge}7$ cycles, as it will be explained in details.

Two possible deviations from Paris' law occur towards either the threshold or towards the static failure region (see Fig. 4), suggesting three regions in the actual crack propagation law. In Stage I (near the threshold, see also Fig. 5), the crack growth rate decreases asymptotically to zero as ΔK approaches a threshold value ΔK_th. This means that for stress intensities below ΔK_th, there is no crack growth, and hence there is a "fatigue threshold". An early attempt to model the near- threshold region came from Donahue et al. [19] as[3]

$$\frac{\mathrm{d}a}{\mathrm{d}N} = C[\Delta\sigma\sqrt{\pi a} - \Delta K_\mathrm{th}]^m. \tag{12}$$

The integration of this law is also possible in closed form, leading to

$$N = \frac{2}{C\pi\Delta\sigma^2}\left[\frac{(\Delta K - \Delta K_\mathrm{th})^{2-m}}{2-m} + \frac{\Delta K_\mathrm{th}(\Delta K - \Delta K_\mathrm{th})^{1-m}}{1-m}\right]_{a=a_i}^{a=a_\mathrm{f}}. \tag{13}$$

For Stage II, Paris' law in Eq. (7) works correctly, up to deviations in Region III (see again Fig. 5) which exhibits a rapidly increasing growth rate towards ductile tearing and/or brittle fracture. For this other deviation, it becomes evident that the toughness condition for the $K_\mathrm{max} = K_\mathrm{Ic}$ is involved, requiring $RK_\mathrm{max} = K_\mathrm{min}$, and hence $\Delta K = K_\mathrm{max}(1-R) = K_\mathrm{Ic}(1-R)$, as proposed first by Foreman et al. [20] and later in combined equations for both high and low ΔK values, for example by McEvily and
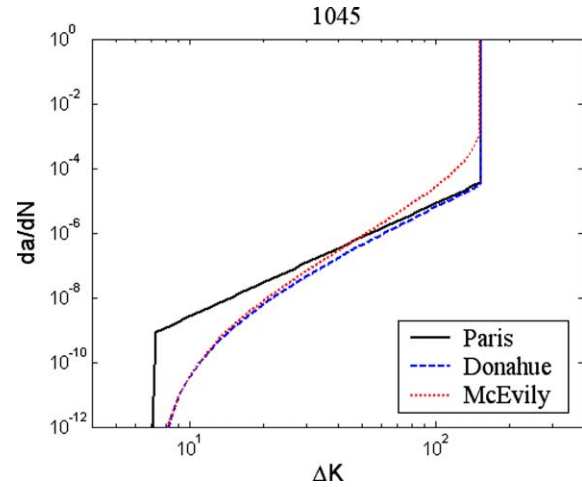

Fig. 4. Qualitative comparison of Paris' law with Donahue et al. [19] and McEvily and Groeger [21] taking for C and m constants the values for SAE1045 in Table 1. Actual fitting of data points may suggest alternative comparisons.
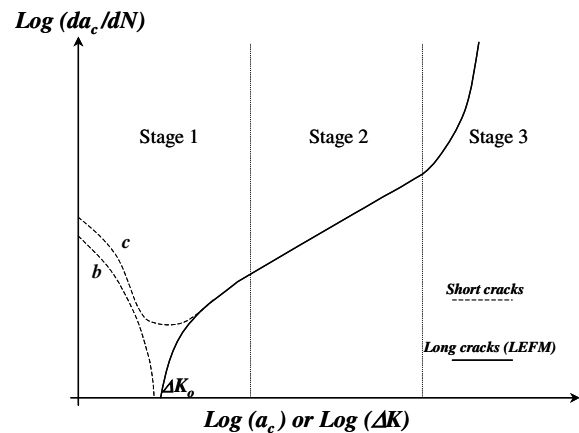

Fig. 5. A schematic of the typical fatigue growth behavior of cracks. "b" and "c" are possible regimes of short cracks.

Groeger [21]. Notice also that these laws tend to show the R-ratio effect only near the K_c, where the dependence of the threshold on R remains implicit in (12) for example, whereas more appropriate laws would need to show the R-dependence on the entire curve.

Notice that the El Haddad equation (2) also permits an interpretation in terms of "reduced" crack propagation threshold. In fact, it can be rewritten as

$$\Delta K_\mathrm{th,sc} = \Delta K_\mathrm{th}\sqrt{\frac{a}{a+a_0}}. \tag{14}$$

This in principle permits to extend the lower limit for the Paris law integration *below* the long crack threshold, making the actual limit that defined by the El Haddad equation itself. However, it should be borne in mind that for short cracks the average crack propagation rate is likely to be much higher than that obtained from the possible extension of the original Paris law. Hence, in our approach, the possi-

---

[3] We are assuming the same power-law intermediate regime (in particular, the same constant C in Eqs. (7 and 12)), but this is not necessarily the only choice when fitting actual data points.

ble regimes on the left of the long crack threshold in the extended KT diagram (i.e. part of region "2" in Fig. 1) will be modeled by the Basquin SN curve – and the transition, with a newly defined "generalized El Haddad" equation.

Fig. 5 shows example realistic crack propagation laws, where the Paris law regime is clearly only obtained in the intermediate region for sufficiently long cracks. A deviation similar to the Donahue correction is also distinguished for long cracks, and two possible deviations from Paris's law for short cracks are indicated as "b" and "c". However, the focus of this paper is on region "3" of Fig. 1 (i.e. short cracks and high stress range), and hence we shall return on the deviations of the map obtained near the threshold (region "1") using the Donahue equations ((12) and (13)), in a later paragraph.

Turning back on the issue of short cracks, they give rise, as also indicated qualitatively in Fig. 5, to multi-valued functions with either acceleration or decelerations with respect to the "reference" Paris power law (Pearson [24], Ritchie and Lankford [25] and Miller [26]). This results possibly in various "minima" in da/dN, and multiple small-crack curves, which depend on micro-structural aspects of crack arrest at grains boundaries (Hobson et al. [27] and Navarro and de los Rios [28]). Hence, while the detailed understanding of these various effects and the development of sophisticated computational models is in progress [27–30], we shall try a much simpler approach, which may be oversimplified in some cases, but which we believe would have the advantage to point out the natural extensions of very popular concepts such as the Kitagawa diagram and the El Haddad equation.

3. Preliminary comparisons

If we compare the propagation life of a pre-cracked specimen, as predicted with the Paris integrated law ((8) and (10)), with the expected life of the uncracked material as predicted with Basquin–Wohler's law ((5) and (7)), we obtain curves such as in the examples in Fig. 6, and for initial crack sizes of $a_i/a_0 = 1, 10, 100, 1000$, and for the steel 1045 in Table 1. The Paris curves are truncated from above, by the static failure level, and from below, by the El Haddad threshold. For $a_i/a_0 = 1, 10$, the Paris curve, particularly in its approximate form (10), actually intersects with the Basquin–Wohler's law ((5) and (6)), and above this level its prediction are clearly in error, suggesting the stress level is too high for it to apply. In fact, below the number of cycles N_t of the transition between the two regimes, failure occurs already for the uncracked material, and the life for a specimen with such a small initial crack cannot be higher. For larger cracks, $a_i/a_0 = 100, 1000$, the final size of the crack gives the critical condition, since static failure becomes dictated by toughness rather than ultimate strength. Hence, as fatigue limit "lowers" the long-crack stress intensity range threshold, to the effective value given by the El Haddad equation (2), then Wohler's
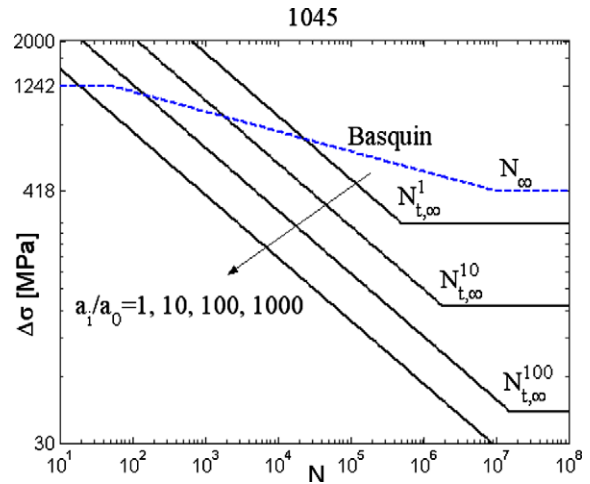

Fig. 6. An example of comparison for Basquin curve (dashed) and the simplified form of the Paris integrated law (10) (solid) for $a_i/a_0 = 1, 10, 100, 1000$. The Basquin line is truncated to the fatigue limit (defined conventionally at 10^7 cycles), whereas the Paris lines are truncated to the El Haddad fatigue limit of Eq. (2).

law "accelerates" the crack propagation rate of the Paris law in region "3" of Fig. 1.

In the literature, we could not find this simple comparison between the Paris and Basquin predictions. Most modifications of Paris's law are attempts to understand the actual *mechanisms* of departure from the ideal conditions or simple ad-hoc modifications for single effects, such as crack closure, short cracks, see for example [22–26], among others. A simple transition has not been attempted in the context of finite life, where the SN behavior of the *uncracked* material moves towards the Paris regime.

The transition from one regime to the other is clearly obtained by equating the two relationships ((5) and (10)) for a given number of cycles, obtaining

$$N_t = \overline{C}\left(\frac{a_i^{2-m/2}}{\left(\frac{m-2}{2}\right)C\overline{C}\pi^{m/2}}\right)^{\frac{k}{k-m}}, \qquad \Delta\sigma_t = \left(\frac{a_i^{2-m/2}}{\left(\frac{m-2}{2}\right)C\overline{C}\pi^{m/2}}\right)^{\frac{1}{m-k}}$$

(15)

or finally in terms of crack size

$$a_t = \left(C\pi^{m/2}(m/2-1)\overline{C}^{m/k}N^{k-m/k}\right)^{\frac{2}{2-m}}.$$

(16)

To get a more precise transition, we need to write the intersection of the curves ((5) and (8)), i.e. including the effect of the final size of the crack. This results in an improved estimate for the transition size:

$$a_t = \left[a_{f,t}^{1-(m/2)} + C\pi^{m/2}(m/2-1)\overline{C}^{m/k}N^{k-m/k}\right]^{\frac{2}{2-m}},$$

(17)

where we define $a_{f,t}$ as

$$a_{f,t} = \frac{1}{\pi}\left[\frac{K_{Ic}(1-R)}{\left(\frac{\overline{C}}{N}\right)^{\frac{1}{k}}}\right]^2.$$
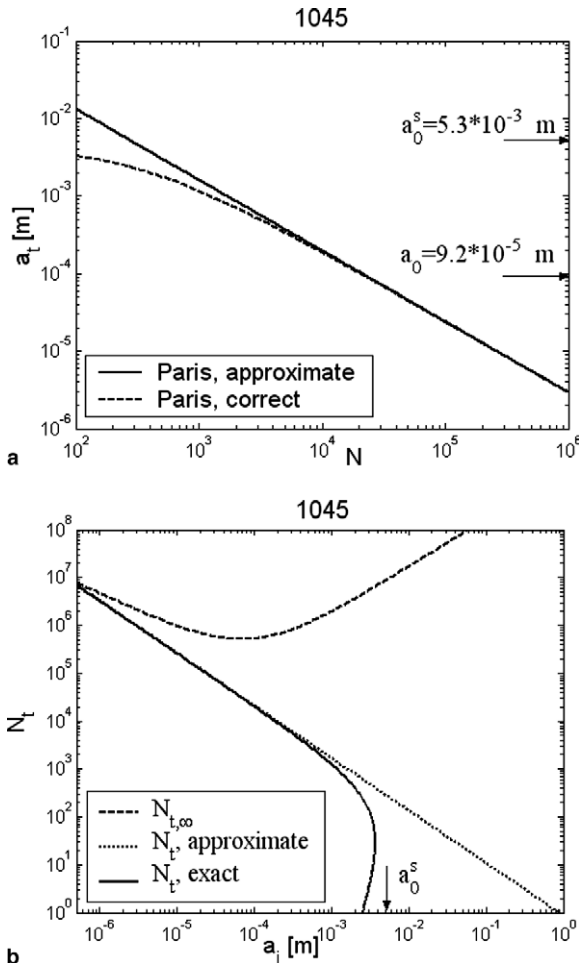
(18)

Fig. 7. (a) The transition size a_t from the Basquin curve to the Paris integrated from Eqs. (16) (approximate) and (17). (b) The transition number of cycles N_t from the Basquin curve to the Paris integrated from Eq. (16) (approximate) and from the solution of Eq. (17) (exact), and $N_{t,\infty}$ from the Paris integrated to the El Haddad threshold from Eq. (19).

For example, Fig. 7a gives the transition size a_t in terms of the expected life, according to Eqs. (16) and (17). It is clear that the approximate Eq. (16) overestimates the correct value of the transition size of Eq. (17). Notice also in the Fig. 7a that the El Haddad "intrinsic" crack size a_0 defined from the fatigue threshold (1) and the corresponding static one are indicated, and do not coincide with the values of the transition size a_t at infinite life and static failure, respectively, because they were obtained from a different approach. In particular, the transition size a_t becomes lower than a_0 already for intermediate lives. This indicates that the definition of a_t as a possible "finite life" flaw-tolerance crack size, may be questionable.

The other interesting transition of regimes is obtained from intersection of the Paris integrated law (10) with the El Haddad threshold (2), obtaining as a function of crack size[4]

---

[4] A more correct equation for the Paris integrated law (Eq. (8)) is really not needed here.

$$N_{t,\infty} = \frac{a_i^{1-(m/2)}(a_i + a_0)^{m/2}}{\left(\frac{m-2}{2}\right)C(\Delta K_{th})^m}.\tag{19}$$

Fig. 7b shows the two transitions in terms of number of cycles as a function of the original crack size (N_t, from Basquin to Paris, and $N_{t,\infty}$, from Paris to the El Haddad threshold).

The curve for N_t starts from $10^{\wedge}7$ cycles since the Basquin law is valid, then rapidly decays to very small number of cycles, to finally disappear completely when a_i becomes comparable to the size a_0^s of the transition from the stress-dominated static failure to the toughness-dominated failure. In the mean time, the curve $N_{t,\infty}$ starts from $10^{\wedge}7$ cycles but decays a lot less rapidly, until it starts growing again, and then reaches values greater than $10^{\wedge}7$ cycles.

4. The KT diagram extended to finite life

Clearly, the importance of the transitions is evident. The transitions defined by N_t and a_t permit to distinguish between a "Basquin–Wöhler" dominated regime to a "Paris"-dominated regime. These two regimes are considered as the natural analogous of the stress range fatigue limit, and the stress intensity range threshold, respectively. A natural extension of the KT diagram for infinite life is then obtained for the finite life, by using this idea. In particular, for very small crack, the Basquin–Wöhler curve condition applies, whereas for larger cracks, namely $a_i > a_t(N)$, the crack propagation law applies for the finite life. Hence, as the original KT diagram can be obtained from the minimum of fatigue limit and fatigue threshold

$$\Delta\sigma_{KT}(a) = \min(\Delta\sigma_0, \Delta K_{th}/\sqrt{\pi a})\tag{20}$$

then the extended KT (KT-Generalized, or KTG as an acronym in the following) for finite life for N can be immediately written as the minimum between Eqs. (5) and (10)

$$\Delta\sigma_{KTG}(N,a) = \min\left((\overline{C}/N)^{1/k}, \left[\left(\frac{m-2}{2}\right)C\pi^{m/2}N\right]^{-1/m}a^{\frac{1}{m}-\frac{1}{2}};\right)\tag{21}$$

where notice the dependence on the initial crack size is the inverse square root expected in the KT diagram, but increased by a factor $1/m$. Obviously, Eq. (21) gives an abrupt transition from the SN curve limit to the Paris integrated curve limit, which can be corrected by adding the transitional size of the crack as "intrinsic crack" a_t, deriving a generalized El Haddad equation (Generalized EH, or EHG) as

$$\Delta\sigma_{EHG}(N,a) = \left[\left(\frac{m-2}{2}\right)C\pi^{m/2}N\right]^{-1/m}(a + a_t(N))^{\frac{1}{m}-\frac{1}{2}}.\tag{22}$$

However, a more precise treatment has to use the full form of the Paris integrated Eq. (8), leading to

$$N_{\text{EHG}} = \frac{2}{2-m}$$

$$\times \frac{1}{C\Delta\sigma^m \pi^{\frac{m}{2}}} \left\{ [a_{\text{f,t}}(N)]^{\frac{2-m}{2}} - (a + a_{\text{t}}(N))^{\frac{2-m}{2}} \right\}. \quad (23)$$

This form of equation is implicit, given a_{t} and a_{f} both depend on the given number of cycles. Hence, one needs to solve (23) for a given N, obtaining a curve of stress range as a function of initial crack size a (later, we shall also see how to use this equation as a SN curve, for a given a rather than for a given N). Fig. 8 shows some example for the usual 1045 steel, including Paris truncated to the El Haddad fatigue limit, as well as the original Basquin law for the uncracked material, and the new EHG in the full form (23) (indicated as "*EHG*") or in the approximate form (22) without consideration of the a_{f} term (indicated as "*EHG, no a_{f}*"). It is clear that the EHG tends to be conservative with respect to the original Paris law, and hence can be considered particularly useful for design purposes. Notice also that the approximate form of EHG (22) is convenient and quite correct for large number of cycles, whereas at low N, the full form is needed (23). This reflects also the fact that the region "3" at low N is the interaction of various regimes, i.e. the original Basquin regime towards the Paris regime and finally toughness failure.

The extended KT diagram may turn out very useful to understand the limits of validity of Paris' law from a new perspective. In fact, as in the derivation of toughness it is well known that a sufficiently large crack and specimen is needed, similar care should be used for Paris' law constants measurement, where the requirements on intermediate points generally would depend on appropriate intermediate conditions. We can also say that the effects of crack propagation rate curves are here given in a different (integrated) plot, which may be convenient to explore the data for design purposes, when the final life is important and not the instantaneous speed of propagation.

Notice also in particular the region for very low applied stress ranges, which shows very long fatigue lives, unless the initial crack is very large. This indicates a possible difficulty in measuring data in this range.

5. The generalized El Haddad equation as a new SN curve

The obtained Eq. (23) can clearly also serve as a new SN curve interpolating between Basquin–Wöhler and Paris regimes. The different regions of the extended KT diagram result in the SN curves of Fig. 9. Notice that, starting from the Basquin "upper" limit, we find that the EHG curve interpolates for the high stress range case. This is generally discussed in the context of deviations from Paris law, since it is known that the two effects (which depend on the size of the crack) are the decay towards the threshold (for long cracks) and the acceleration for short cracks well below the long-crack threshold and well above the level of the Paris law — this second effect is what we modeled with the EHG curve, the former with the Donahue curve.

This is shown in the following Fig. 9 for the usual example material, and for $a_i/a_0 = 1, 10, 100, 1000$. Notice in particular that for low $a_i/a_0 = 1, 10$ the transition given by the generalized EH equation (23) interpolates between the Basquin–Wöhler and the Paris regimes, and is rather abruptly truncated at the fatigue threshold. For larger $a_i/a_0 = 100$, 1000, the static failure condition is given by the toughness condition, and no longer by the Basquin–Wöhler law (5). Hence, the starting point is Paris law in its full formulation of Eq. (8), i.e. taking the final size of the crack into account. This transition however occurs naturally in the generalized El Haddad in its full form (23).

6. Further equations near the fatigue threshold

In the derivations of the new generalized El Haddad equations, we have assumed as a basic crack propagation curve, the original Paris power law curve (7). We return
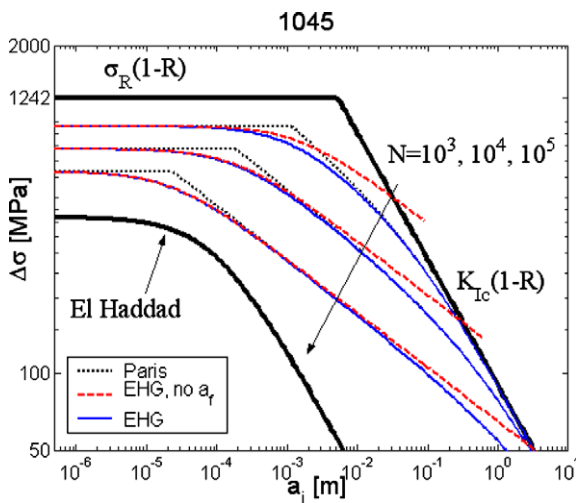

Fig. 8. The extended KT diagram with EHG equation (23) or EHG approximate form (22), as compared to the integrated Paris in the full form (8), truncated to the Basquin law (5) level.
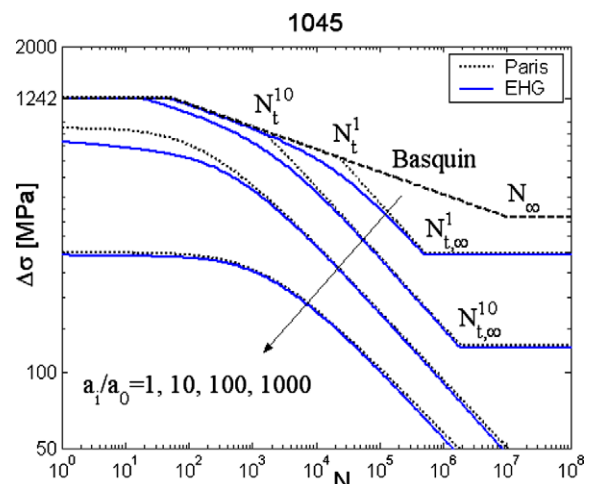

Fig. 9. The SN curves obtained with the generalized EH (Eq. (23)), and Paris (8), for $a_i/a_0 = 1, 10, 100, 1000$.

now to the issue of deviations from the power law regime, in particular near the threshold, using for example the Donahue et al. equations ((12) and (13)). It should be borne in mind that the form given with the same Paris constants (C, m) of the Paris law, clearly shows slower propagation rates than the simpler Paris law, and hence the generalized El Haddad equations so far obtained remain a conservative, simpler approach. In the generalized El Haddad equation obtained (23), as confirmed by the curves of Fig. 9, gives essentially the transition from the Basquin–Wöhler to the Paris regime (for small initial crack sizes) or directly from the Paris law in its full form depending on the final crack size. The Donahue curve ((12) and (13)) following the same reasoning, can be extended into another generalized El Haddad form, by defining a new transition crack size from the intersection of the Basquin–Wöhler curve at a given number of cycles, to the corresponding Donahue curve. The expression is not obtained in closed form and hence will not be given here. Further, by adding this size to the initial crack size in Eq. (13), the new equation is obtained, as plotted in Fig. 10a in the generalized KT diagram, or as a new SN curve, in Fig. 10b. The resulting expression, as expected, is a smoother transition than the simpler EHG equation (23), particularly as a SN curve in the transition towards the fatigue threshold. Notice also that in Fig. 10c the transition size is given for the Donahue equation, noting that the principal difference is obtained towards the small values of crack sizes, since this tends here towards the a_0 value.

7. Other materials

So far, we have only presented maps elaborated on the 1045 steel. Other materials having $m > 2$, like the steel A588 in Table 1, would show similar behavior. More differences would be present for materials having $m < 2$, like the steel RQT501 and RQT701 in Table 1. We present in fact in the following Fig. 11, the resulting maps for the other 3 steels, showing that the case of steel RQT501 and RQT701 is very different from the previous two steels. In particular, there seems to be a much large region of possible propagation, because of the very high number of cycles attained before the crack reaches the critical size. In fact, in the integrated form of the Paris equation, namely Eq. (8), not only it is no longer possible to neglect the effect of the initial size, but actually the shape of the entire contour line depends critically by the effect of the difference between the two terms, that involving the initial crack size, and than involving the final crack size. As a consequence, the intersection of the Basquin line and the Paris line (i.e. the transition size a_t) is so high that most of the generalized El Haddad contour lines are concentrated towards the toughness failure line. Also, notice for values above a certain life, namely $N = 10^5$ cycles in this example, the intersection does not exist, which makes the Paris lines to cross the El Haddad equation (2) for the threshold. For this reason, and also to keep consistency with the previous plots, we do not show
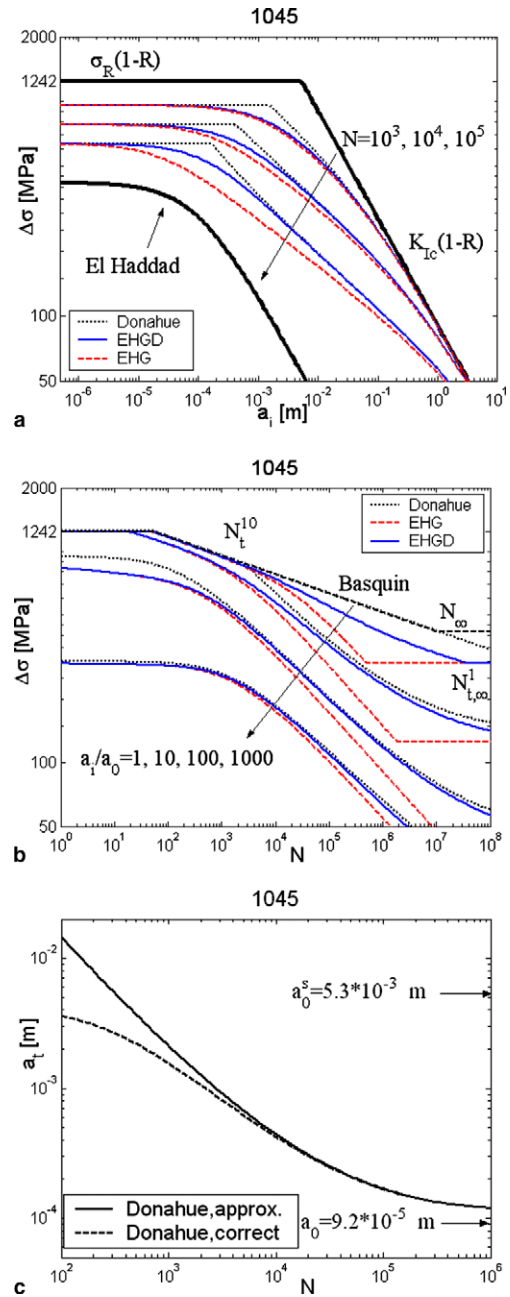

Fig. 10. The fatigue map (a) and fatigue SN curves (b) obtained with the generalized EH (Eq. (23), using Paris), or the Donahue equation for $a_i/a_0 = 1, 10, 100, 1000$. Finally (c) is the crack size transition size a_t for the Donahue equation.

lines above $N = 10^5$ cycles (also consistently with the previous cases for the other materials).

Fig. 12 shows the resulting SN curves, again for the 3 steels, and here we can see that materials with $m < 2$ show a very "concentrated" decrease of fatigue strength towards the high number of cycles.

8. Discussion

The "asymptotic matching" practice of a *fictitious* increase of the crack size, used in the El Haddad equation
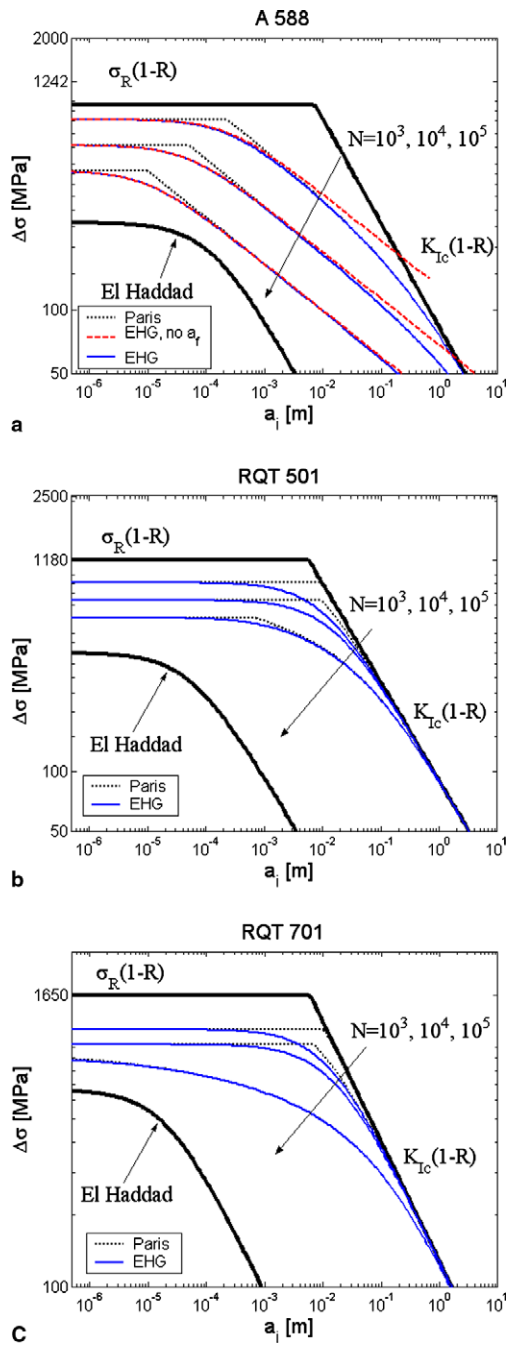
Fig. 11. The fatigue map obtained with generalized EH (Eq. (23)) for the other materials in Table 1, as compared to the integrated Paris (8), truncated to the Basquin law level.
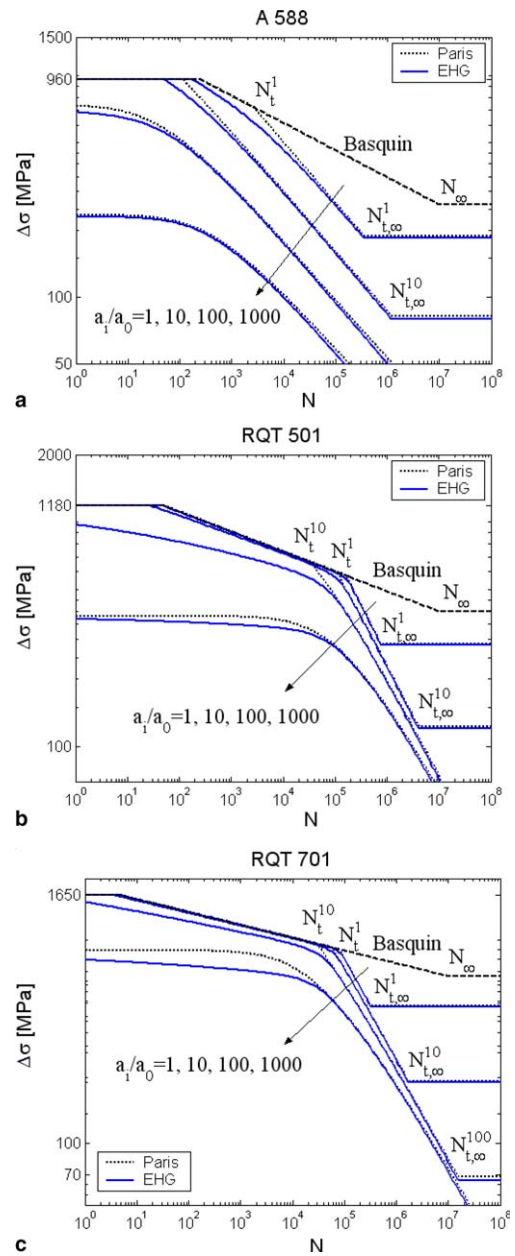

Fig. 12. The fatigue SN curves obtained with generalized EH (Eq. (23)) for $a_i/a_0 = 1, 10, 100, 1000$, as compared to the integrated Paris (8), truncated to the Basquin law level.

(2), and its newly derived generalized form (23), corresponds also qualitatively to the Dugdale strip-yield concentrated plastic damage models which have been developed for fatigue by Newmann [30–32] and Nguyen et al. [33], or Desphande et al. [34] among others. Accurate models in principle should capture the delicate interplay between bulk cyclic plasticity, closure (possibly all mechanisms of closure, such as plasticity-induced or roughness-induced or others), and gradual decohesion at the crack tip. The increase of the crack could be considered proportional to

the "instantaneous" cyclic yield zone and appropriate "constraint factors" could be defined to account for the transition from flat-to-slant crack growth, i.e. from plane-strain conditions at low stress-intensity factors, to plane stress as the plastic-zone size becomes large compared to thickness. The capability to take into account of local and instantaneous plastic properties of the material, and of geometrical and shape factors, make these models potentially very accurate, but also very complicated, requiring a significant amount of computational effort and additional knowledge of material properties (particularly, of plastic cyclic hardening, as for example present models simply use perfect plasticity). Our approach should

not be considered as a direct alternative to these sophisticated simulations, but a perhaps less quantitative, simpler route for qualitative discussion and design maps.

Various authors have suggested classifications of short cracks (see Ritchie and Lankford [35], or Miller [26]) into (i) *microscopic short crack* ("microstructurally small", for which continuum mechanics breaks down and Microstructural Fracture Mechanics is needed, see for example the models of Hobson et al. [36] and later Navarro and de los Rios [28]; this is perhaps the most complex category, since crack deceleration or self-arrest are very dependent on the grains size and orientations, and possible acceleration decelerations or "minima" in da/dN and multiple small-crack curves can be found (Ritchie and Lankford [25]). (ii) *physically small crack* ("mechanically small" compared to the scale of local plasticity, for which Elastic–Plastic Fracture Mechanics (EPFM) is needed, first introduced by Tomkins (see Miller, [26]), who equated da/dN to crack tip decohesion (from knowledge of the cyclic stress–strain curve), and thence to the bulk plastic strain field such as occurs, for example, under high strain fatigue. Further generalizations of our model could also be considered to incorporate these definitions and alternative formulation in the extended Kitagawa diagram.

Finally, two other remarks on possible connections with existing literature, partly suggested by one referee. Firstly, we should mention that the static equivalent of the El Haddad equation (2) has been already proposed by some authors (see, for example [37–39]) and is the basis for the size scale effect studied for large structures. Secondly, there are various approaches proposed to obtain the initiation life from a Basquin–Coffin–Manson type of equation (which, however, needs to be "extracted" in the sense of initiation of a crack, and not of final failure), and summing this to the propagation life using Paris law:

(1) In the specific context of fatigue of welded structures [40–43], often it is *assumed* that the transition occurs at a given, fixed, size of the crack (0.25 or 0.15 mm).

(2) In the generic case of notched member [44], the stress ahead of the notch, which is decreasing, is used to estimate the da/dN crack initiation rate from Basquin–Coffin–Manson, and the crack propagation curves da/dN from Paris law. When the two lines cross, it is assumed that crack propagation dominates.

However, these two Initiation-Propagation (IP) approaches are rather different from our approach, and a detailed comparison is quite difficult: in the former case, the assumption of a given size for crack initiation is somewhat arbitrary. Even assuming a Coffin–Manson law can be used to define "initiation" in the sense of generation of a crack of length 0.25 or 0.15 mm, then it is not necessarily true that Paris law can be used for cracks of this size, because, for example, for large enough applied stress range, EPFM is needed even at this sizes. On the other hand, at low enough applied stress range, this arbitrary initial crack size may not be sufficient for crack propagation to start (since the product of stress range and square root of crack size may be well below the long crack fatigue threshold). The fact that this approach is used mainly with the welded joints problem may be due to the fact that welded joints have intrinsic long cracks introduced by the welding process, and hence their fatigue life has more to do with propagation in the Paris law sense than with initiation. If this is the case, one really would need to define this "critical size" for initiation accurately and appropriately (and not just 0.25 or 0.15 mm as probably appropriate only for some typical classes of welded joints), and yet it is not entirely clear if the idea of summing initiation and propagation leads to the correct shape of the SN curve (particularly at HCF), as Hou and Charng [43] themselves recognize: "*it is still controversial whether the SN curve of welded joints becomes less steep at a high cycle regime as is commonly seen in the calculated SN curves of the IP model*". We suppose that in fact, if our picture above is correct, i.e. if the "fatigue limit" of the welded joint has more to do with a transition to the fatigue threshold, then the slope in the area of HCF has nothing to do with the initiation slope as suggested by the IP approach. The IP approach basically assumes that we can record or experimentally evaluate the occurrence of a crack of a given size (by strain gages or other means) and we can use a unique "initiation" Coffin–Manson law, i.e. not recognizing the initial defects in the material (with their variability), essentially requires a different law – this is recognized by the authors of Ref. [43] who admit there is large scatter in the results of initiation.

In the latter case, the use of a law derived with an unnotched specimen to estimate the initiation life of a notched one locally is again somewhat arbitrary. What we are proposing is rather a *comparison* between the Basquin curve for the uncracked material, and the Paris curve neglecting short crack effects. The interpolation between the two gives a "map" by filling the missing information in the simplest possible way, i.e. by interpolation between the well known regimes.

9. Conclusions

We have proposed new diagrams and new equations, generalizing the Kitagawa–Takahashi diagram and the El Haddad equation, respectively, to finite life. In particular, in the absence of geometrical effects and for constant amplitude loading, a general equation (Eq. (23)) has been obtained for fatigue life by interpolating between the Basquin–Wöhler's law for the uncracked material and the Paris integrated equation, either in a simplified form, independent on the final size of the crack, or in its full form, which permits to take into account also of possible regime of static toughness failure. The resulting expression can also be seen as a SN curve, for a given initial crack size, and has the merit to show the various transitions between

known regimes from a new perspective. Also, as an empirical equation, it does not contain explicit description of physical mechanisms, but being an interpolation procedure, it does not have the risks associated to the inevitable "extrapolation" nature of the many other phenomenological but essentially empirical models. The new generalized El Haddad equation deals with the regime of short cracks and high stress range values, whereas a second equation obtained starting from the Donahue correction of the Paris law, suggests the deviations near the threshold, which, however, can be avoided considering the simpler generalization of the El Haddad equation as a conservative estimate for design purposes.

References

[1] Kitagawa H, Takahashi S. Applicability of fracture mechanics to very small cracks or cracks in the early stage. In: Proceedings of the second international conference on mech. behaviour of matls., ASM; 1976. p. 627–31.

[2] Paris P, Gomez M, Anderson W. A rational analytic theory of fatigue. The Trend Eng 1961;13:9–14.

[3] Paris P, Erdogan F. A critical analysis of crack propagation laws. J Basic Eng, Trans Am Soc Mech Eng 1963;December:528–34.

[4] El Haddad M, Topper T, Smith K. Prediction of non-propagating cracks. Eng Fract Mech 1979;11:573–84.

[5] Atzori B, Meneghetti G, Susmel L. Material fatigue properties for assessing mechanical components weakened by notches and defects. Fat Fract Eng M 2005;28(1–2):83–97.

[6] Venkateswaran P, Raman SGS, Pathak SD. Generation of stress vs. crack length plots for a ferritic steel weld metal based on Kitagawa–Takahashi approach. Mat Lett 2005;59(4):495–8.

[7] Peters JO, Boyce BL, Chen X, et al. On the application of the Kitagawa–Takahashi diagram to foreign-object damage and high-cycle fatigue. Eng Fract M 2002;69(13):1425–46.

[8] Araujo JA, Nowell D. Analysis of pad size effects in fretting fatigue using short crack arrest methodologies. Int J Fat 1999;21(9):947–56.

[9] Atzori B, Lazzarin P. A three-dimensional graphical aid to analyze fatigue crack nucleation and propagation phases under fatigue limit conditions. Int J Fract 2002;118(3):271–84.

[10] Atzori B, Lazzarin P, Meneghetti G. Fracture mechanics and notch sensitivity. Fat Fract Eng M 2003;26(3):257–67.

[11] Rodopoulos CA, Choi JH, de los Rios ER, Yates JR. Stress ratio and the fatigue damage map. Part I. Modelling. Part II. The 2024-T351 aluminium alloy. Int J Fat 2004;26(7):739–46. p. 747–52.

[12] Fleck NA, Kang KJ, Asbhy MF. Overview 112: the cyclic properties of engineering materials. Acta Metal Mater 1994;42:365–81.

[13] Suresh S. Fatigue of materials. Cambridge: Cambridge University Press; 1998.

[14] Polák L. Plastic strain-controlled short crack growth and fatigue life. Int J Fat 2005;27(10–12):1192–201.

[15] Murakami Y, Harada S, Endo T, Tani-ishi H, Fukushima Y. Correlations among growth law of small cracks, low-cycle fatigue law and applicability of Miner's rule. Eng Fract Mech 1983;18(5):909–24.

[16] Murakami Y, Miller KJ. What is fatigue damage? A view point from the observation of low cycle fatigue process. Int J Fat 2005;27:991–1005.

[17] Nisitani H, Goto M, Kawagoishi N. A small-crack growth law and its related phenomena. Eng Fract Mech 1992;41(4):499–513.

[18] Nisitani H, Goto M. A small crack growth law and its application to the evaluation of fatigue life. In: Miller KJ, de los Rios ER, editors. Behaviour of short fatigue cracks. Mech. Eng. Publishers; 1987. p. 461–78.

[19] Donahue RJ, Clark HM, Atanmo P, et al. Crack opening displacement and the rate of fatigue crack growth. Int J Fract Mech 1972;8:209–19.

[20] Foreman RG, Kearney VE, Engle RM. Numerical analysis of crack propagation in cyclic-loaded structures. J Basic Eng 1967;89:459–64.

[21] McEvily AJ, Groeger J. On the threshold for fatigue-crack growth. In: Fourth international conference on fracture, vol. 2, University of Waterloo Press, Waterloo, Canada; 1977. p. 1293–298.49.

[22] Laird C. Mechanisms and theories of fatigue. In: Fatigue and microstructure. American Society for Metals; 1979. p. 149–203.

[23] Elber W. Fatigue crack closure under cyclic tension. Eng Fract Mech 1970;2:37–45.

[24] Pearson S. Initiation of fatigue cracks in commercial aluminum alloys and the subsequent propagation of very short cracks. Eng Fract Mech 1975;7:235–47.

[25] Ritchie RO, Lankford J, editors. Small fatigue cracks. Warrendale: The Metallurgical Society of the American Institute of Mining, Metallurgical and Petroleum Engineers; 1986.

[26] Miller KJ. A historical perspective of the important parameters of metal fatigue and problems for the next century. In: Wu XR, Wang ZG, editors. Proceedings of the 7th international fatigue congress (Fatigue'99). Beijing: Higher Education Press; 1999. p. 15–39.

[27] Hobson PD, Brown MW, de los Rios ER. In: Miller KJ, de los Rios ER, editors. EGF (ESIS) Publication No. 1, The behaviour of short fatigue cracks. London: Mechanical Engineering Publications; 1986. p. 441–59.

[28] Navarro A, de los Rios ER. A microstructurally short fatigue crack growth equation. Fat Fract Eng Mater Struct 1988;11:383–96.

[29] Kitagawa H, Tanaka T, editors. Fatigue 90. Birmingham: Materials and Components Engineering Publications; 1990.

[30] Newman Jr JC. The merging of fatigue and fracture mechanics concepts: a historical perspective. Prog Aerospace Sci 1998;34:347–90.

[31] Newman Jr JC, Phillips EP, Swain MH. Fatigue-life prediction methodology using small-crack theory. Int J Fat 1999;21:109–19.

[32] Newman Jr JC, Brot A, Matias C. Crack-growth calculations in 7075-T7351 aluminum alloy under various load spectra using an improved crack-closure model. Eng Fract Mech 2004;71:2347–63.

[33] Nguyen O, Repetto EA, Ortiz M, Radovitzky RA. A cohesive model of fatigue crack growth. Int J Fract 2001;110:351–69.

[34] Deshpande VS, Needleman A, Van der Giessen E. Discrete dislocation modeling of fatigue crack propagation. Acta Materialia 2002;50:831–46.

[35] Ritchie RO, Lankford J. Small fatigue cracks: a statement of the problem and potential solutions. Mater Sci Eng 1996;84:11–6.

[36] Hobson PD, Brown MW, de los Rios ER. In: Miller KJ, de los Rios ER, editors. EGF (ESIS) Publication No 1, The behaviour of short fatigue cracks. London: Mechanical Engineering Publications; 1986. p. 441–59.

[37] Bazant ZP. Size effect on structural strength: a review. Arch Appl Mech 1999;69:703–25.

[38] Seweryn A. Brittle fracture criterion for structures with sharp notches. Eng Fract Mech 1994;47:673–81.

[39] Taylor D, Cornetti P, Pugno N. The fracture mechanics of finite crack extension. Eng Fract Mech 2005;72:1021–38.

[40] Lawrence FV. Estimation of fatigue-crack propagation life in butt welds. Welding Res 1973;52(Supplement):401–9.

[41] Ting JC, Lawrence FV. A crack closure model for predicting the threshold stresses of notches. Fat Fract Eng Mater Struct 1993;16:93–114.

[42] Ting JC, Lawrence FV. A crack closure model for predicting the threshold stresses of notches. Fat Fract Eng Mater Struct 1993;16.

[43] Hou C-Y, Charng J-J. Models for the estimation of weldment fatigue crack initiation life. Int J Fat 1997;19(7):537–41.

[44] Socie DF, Morrow J, Chen WC. A procedure for estimating the total life of notched and cracked members. J Eng Fract Mech 1979;11:851–9.